

ALMA Memo No 348

A Preliminary ALMA Zoom Array Design for the Chanjnantor Site.

John Conway
Onsala Space Observatory, Sweden

February 15th, 2001

Abstract

I present a preliminary zoom array design for ALMA fitted into the the Chanjnantor site, and compare its properties with the proposed double ring strawperson array. Both arrays have virtually the same number of pads and require almost the same number of antenna moves. To first order the two arrays are shown to have similar radial distributions of baselines, although the coverage of the zoom array is smoother and is slightly more centrally condensed. For snapshots the peak sidelobes for the two styles of array are similar. However the zoom array has 40% smaller peak sidelobes for long track observations. For both snapshots and long tracks the degree of uv cell occupancy for the two arrays is very similar. We argue that zoom arrays will have slightly smaller or equal phase noise effects than dual ring arrays of the same resolution. For the zoom array we show that North-South extended array configurations with low sidelobes exist for observing Northern hemisphere or South polar sources.

The zoom array is a very flexible design, which can accommodate many different modes of operation. It can for instance be operated as set of fixed arrays like the double ring,

with the important difference that the sizes and numbers of configurations are variable. Alternatively the array could be operated in a continuous reconfiguration mode with perhaps six antennas being moved per week. This mode of operation has some astronomical advantages and significant operational advantages. However the array is operated, if antenna moves are prevented by bad weather, the zoom array is always left in a configuration with a good uv coverage without stranded 'outlier' antennas.

After a certain amount of convergence the two styles of array proposed for the intermediate configurations are no longer dramatically different. However in almost all performance areas we argue that the zoom array is slightly superior. This combined with its much greater flexibility suggests that the zoom array design should be chosen for the intermediate configurations. Put another way - we find no strong argument in favour of (and several against) building particular scale lengths into the array design as is done in the dual ring design.

CONTENTS

[1. Introduction:](#)

[2. Zoom Array Design:](#)

[2.1 Intermediate Spiral:](#)

[2.2 Compact Array:](#)

[2.3 Outer Ring:](#)

[2.4 Sidelobe Optimisation:](#)

[3. Array Description:](#)

[3.1 A-Array Equivalent:](#)

[3.2 B-Array Equivalent:](#)

[3.3 B/C-Hybrid Array:](#)

[3.4 C-Array Equivalent:](#)

[3.5 D-Array Equivalent:](#)

[3.6 E-Array Equivalent:](#)

[4. Comparisons with Double Ring Array: UV Coverages and Beams](#)

[4.1 Snapshot UV density distribution](#)

[4.2 Snapshot UV coverages and Dirty Beams](#)

[4.3 Long track uv densities](#)

[4.4 Long track dirty beams](#)

[4.4 Imaging Simulations](#)

[5. Comparisons with Double Ring Array: Operational](#)

- [5.1 Array Flexibility](#)
- [5.2 Operational Issues](#)
- [5.3 Hybrid Arrays](#)
- [5.4 Fitting the array into the Site.](#)
- [5.5 Roads and Conduits.](#)
- [5.6 Combined Array Imaging](#)
- [5.7 Mosaicing](#)
- [5.8 Pointing Errors](#)
- [5.9 Phase Noise](#)
- [5.10 Tapering.](#)
- [5.11 Inverse Tapering and Super-resolution](#)

[6. Summary](#)

[7. Future Work](#)

1. Introduction:

A number of recent memos have discussed possible ALMA array configurations. For the best possible imaging certain properties are clearly desirable including 1) low sidelobes for snapshot and synthesised beams. 2) Good uniform filling of the uv plane and 3) A wide range of sampled baseline lengths. Unfortunately to some extent these properties are mutually inconsistent which makes the optimisation problem poorly defined. In addition there are important practical and operational constraints. For ALMA as with any other array these constraints are likely to play a deciding rule in the array geometry. Amongst the constraints are that the array must fit into the available terrain and that it should minimise construction and operations costs. These goals can be achieved by sharing as many pads between different configurations as possible. Such pad sharing both minimises the antenna pads and other infrastructure to be constructed and minimises the number of antenna moves needed to go through all configurations

Motivated primarily by the need to minimise infrastructure requirements Conway(1998, memo 216) proposed an array design on a self-similar three armed spiral pattern. In addition to its high degree of pad re-use it was found that this array had excellent uv coverage properties. By a remarkable coincidence for certain spiral parameters the snapshot uv coverage was found to have a distribution close to Gaussian. Similar zoom concepts were developed independently by Webster(1998, memo 233) who noted that any continuously scalable array must have a pad density distribution which scales as $1/r^2$. It was argued by Conway(1999, memo 260) that an initial generating geometry based on a spiral pattern had advantages compared to other $1/r^2$ generating distributions such as multiple nested circles or random distributions. Both Conway(1998, memo 216) and Webster(1998, memo 233) noted that the continuous self-similarity property of a zoom array allowed it to be operated in a wide range of operational modes. It could for instance be operated as a set of conventional fixed configurations or alternatively in a continuous 'zoom' mode. In this second mode a few antennas are moved every few days and the array would gradually change in resolution. Comparisons of the relative efficiencies of continuous and conventional 'burst' reconfiguration showed that that the

continuous mode could in fact be slightly more efficient (Guilloteau 1999, memo 274, Yun 1999, memo 277, and Conway 2000a, memo 283). A first attempt was made by Conway(2000c, memo 292) to fit a zoom spiral array into the Chanjantor site; this early sketch we will refer to as the 'zoom1' design. This present memo present a more complete ('zoom2') design. Specifically it has parameters, including the positioning of the centre of the array allowing it to be directly compared to competing 'dual ring' designs (Yun and Kogan 2000, memo 320). We describe this design in detail starting in Section 3. A subsequent memo will produce a 'zoom3' design whose centre is optimised to the site.

In parallel with the development of zoom arrays described above Kogan, Yun and others have been developing arrays based on double ring or donut distributions of antennas. The focus initially was on developing optimum designs for a single configuration. These arrays were optimised using an algorithm developed by Kogan which iteratively adjusted the antenna positions in order to reduce the peak beam sidelobe. For ratios of of inner to outer radii of 1.1 to 1.5. relatively uniform filling of the uv plane was achieved simultaneously with low (<5%) peak sidelobes. In order to increase the degree of pad sharing between different configurations a strawperson design has been proposed (Yun and Kogan 2000) consisting of a set of concentric rings, with adjacent rings having a ratio 2.1 in radius. In any given configuration two rings would be occupied. When reconfiguring to the next smallest array size the antennas on the outer ring would be moved to the next smallest unoccupied ring. In this way 5 fixed configurations each a factor of 2.1 apart in resolution could cover all array sizes out to 3km. Aspects of this design, in particular the most compact array and the outer ring have also been used in the zoom strawperson design (see Section 2). Furthermore in Section 3 we compare in detail the properties of this double ring strawperson with the zoom spiral array.

Both the 'zoom2' design presented in this memo and the Yun and Kogan (2000) 'Dual ring' design are currently being evaluated for their imaging performance in a series of tests using simulated source distributions. See [Heddles Simulation Page](#).

2. Zoom Array Design :

2.1 Intermediate Spiral :

The strawperson zoom array design is based on a modified three armed logarithmic spiral. We began by considering the uv coverages and beams of geometrically perfect spirals. We investigated how beam sidelobes and uv coverage changed as the pitch angle and spacing of antennas along each arm was varied. We then chose geometrical parameters which gave minimum sidelobes and uv coverages whose radial density was close to Gaussian. In order to allow a more circular beam at a range of elevations a 10% North-South stretch was added to the spiral pattern as advocated by Helfer and Holdaway (1998, memo 198).

2.2 Compact Array :

At both the shortest and longest baselines the geometry was modified from the spiral. On the smallest scales this must be done because of the finite size of the antennas. One approach presented by Conway (2000a, memo 283) was to smoothly convert the log-spiral into an

archimedian spiral at small radius. Although this can give rise to a very compact array with high packing density, it requires a large number of pads and has difficulty with access to the antennas at the centre of the array. As a replacement we used the design presented by Yun and Kogan (2000, memo 320) of a ring of antennas with others inside. This array has advantages of antenna access and has already been optimised to have minimum sidelobes anywhere within the primary beam.

2.3 Outer Ring :

At the opposite extreme of the long baselines it is clear that any array design should strive for the highest resolution given the available terrain. For the Chajnantor site there is relatively flat area of about 3km diameter; given this the highest resolution array should have pads distributed around the outer perimeter of this area. Given this the zoom array was designed to smoothly merge into an outer circle of 3km diameter. Again it was convenient to borrow the outer ring of antennas developed for the double ring array (Yun and Kogan 2000) since this had already been fitted into the terrain. The choice of this outer ring then fixed the centre of the array. The next step was to find the rotation angle of the spiral such that the minimum number of pads landed in areas 'blanked out' in the 5° degree gradient terrain mask. Those few pads in unsuitable terrain were then moved to the nearest valid position.

2.4 Sidelobe Optimisation:

The next step in array design was to use a variant of the Kogan sidelobe minimisation algorithm to optimise the pad positions. It has been shown (Conway 1998, memo 216) that adding some perturbations in pad positions from a geometrically perfect pattern is desirable to reduce sidelobes. Some perturbations are of course forced by the need to avoid bad terrain, but additional perturbations are useful in reducing sidelobes. In making the optimisation some patterns of pad occupancy had to be assumed. The zoom array concept of course allows a very wide range of such pad occupancy patterns. Since however one objective was to make a direct comparison with the double ring strawperson we optimised using pad occupancy patterns which matched the five arrays (A-E) of the double ring strawperson. We chose in each case occupied pad configurations so that the resolution and shortest sampled baseline was the same between the two styles of array. Having done this we started with our D-array equivalent allowing pads to be moved which were occupied in D array but in E. We then optimised for the C-array moving pads occupied in C array but not D etc, etc.

The optimisation routine used was a variant of the Kogan one. Explicitly the peak amplitudes of the electric field synthesised beam (FT of the antenna pattern not uv coverage) were found; this is appropriate since the peaks of the normal power synthesised beam are simply the amplitude of this squared minus a constant. Changes in pad positions were found which simultaneously reduced the 5 - 20 largest peaks in the beam. Several iterations of the beam minimisation process were applied optimising within a radius of 20 beams, which was the same limit used in optimising the double ring arrays (Yun and Kogan 2000). For the zoom design it was possible to reduce the peak sidelobes to between 4% and 6% for all of the A,B,C,D,E equivalent arrays. As described in Section 4.2 these peak sidelobes are very similar to those achieved on optimising the ring arrays. Also in both cases the final optimised array is similar in overall shape to the starting

array. Both these results suggest that the optimisation routines are finding local rather than global minima.

3. Array Description :

As noted in the Introduction the zoom array allows a wide range of possible modes of operation. It can be operated as a conventional set of fixed arrays, where the number and size of the arrays can be decided and/or changed after construction. However, the zoom array can also be operated as a continuously evolving array with one or two antennas moved per day, in which case (see Conway 2000a) there would effectively be 40 different configurations. It is impossible here to show all possible arrays, instead we concentrate on arrays which are equivalent in resolution to the A,B,C,D,E arrays of the strawperson double-ring designs. These are somewhat special choices for the zoom array only in that sidelobe optimisation has been explicitly run for these arrays. In fact we find that circularly symmetric arrays which are intermediate in resolution between say B and C, have peak isolated sidelobes only 50% larger compared to the peak sidelobes in the optimised A,B,C,D and E arrays. Furthermore these increased peak sidelobes occur on isolated far sidelobes. In addition to circularly symmetric arrays suitable for observing equatorial sources the zoom spiral design also naturally allows hybrid arrays of excellent quality (see Section 3.3). These arrays which are extended in the North-South direction are suitable for observing Northern hemisphere or far Southern sources.

3.1 A-Array Equivalent:

Figure 1a shows the distribution of occupied pads in the A-array. Half of the antennas are on the outer ring. Most of the rest are on the outer part of the intermediate spiral, However in order to provide the shortest baselines (down to 79m) some of the pads on the 150m ring are also occupied. Grouping the antennas at the centre has the advantage that the maximum number of short spacings are produced for the minimum number of antennas, and also reduces the number of antenna moves slightly since these antennas need never be moved. A disadvantage is that it causes a ring of higher uv point density in the otherwise smooth uv coverage (see Figure 1b). The effect on the snapshot and long track beams (see Fig 1c) is however fairly benign, in fact the higher density uv ring adds a contribution to the dirty beam which partly cancels out the first sidelobe caused by the fairly abrupt edge of the uv coverage. An alternative way to produce short spacings which should be investigated is to group some of the pads on the outer ring or intermediate spiral closer together.

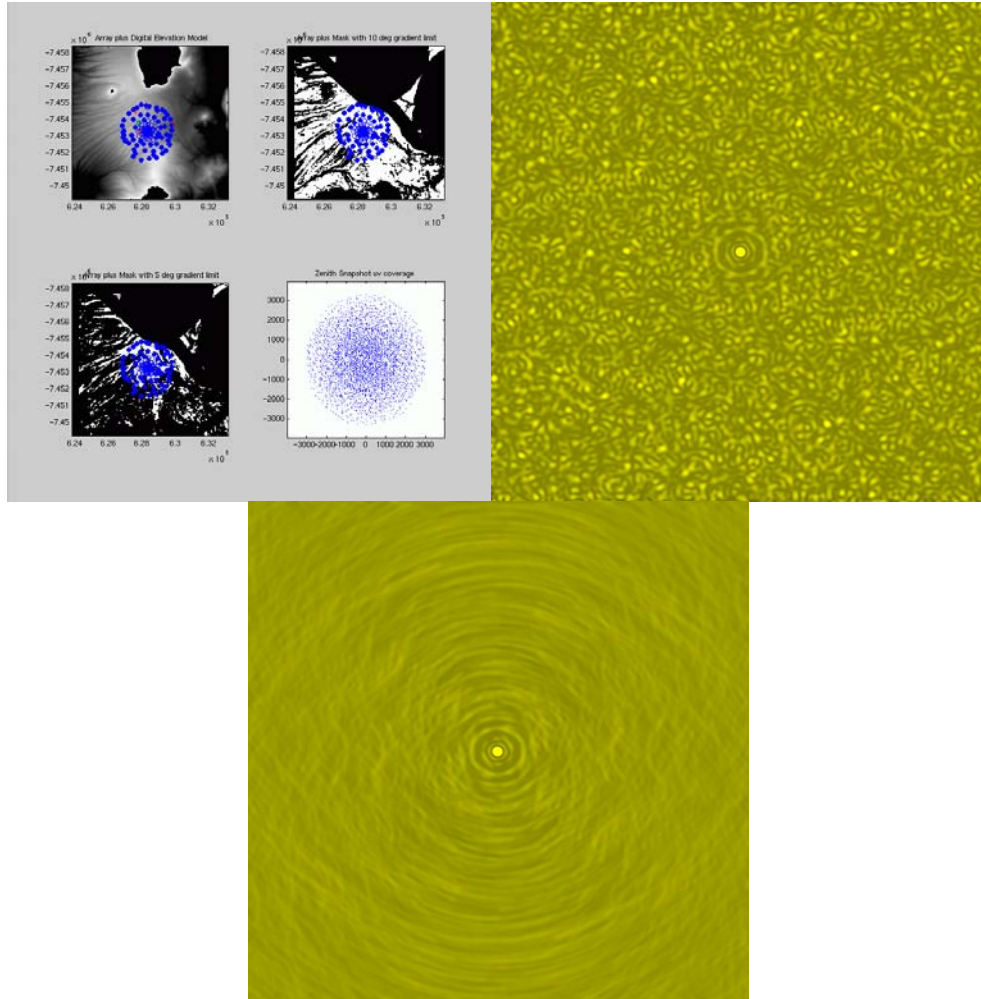


Fig 1(left panel) Pad distribution superimposed onto terrain and uv coverage for A-array equivalent. including histogram of uv baseline lengths. (Middle panel) Zenith snapshot dirty beam. The plotted grayscale ranges between -5% and +10%. The peak sidelobe between radii of 1 and 22 beams is 0.0618. (Right panel) Long track dirty beam for a dec=-23 sources observed +/-2hrs from transit. Note all antennas weights are assumed equal and image is naturally weighted. The peak sidelobe within 20 beams is 0.0259.

3.2 B-Array Equivalent:

After moving half of the antennas inward we obtain the array shown in Figure 2a,b,c, which has a FWHM approximately twice that of the A-array equivalent. Now there are no antennas on the outer ring, most are on the intermediate spiral. A few more antennas are added to the 150m ring so that the minimum baseline is now 32m. As shown in Fig2c the distribution of baseline lengths is very close to gaussian. The result is that the main lobe of the synthesised beam is also close to a gaussian (se Fig 2c) with very small near-in sidelobes. The largest sidelobe within 20 beams is 4.56% an occurs at an isolated peak. In going to long tracks these far out sidelobes are greatly reduced and the 4hour long track beam has a peak sidelobe anywhere within 20 beams of 2.15%.

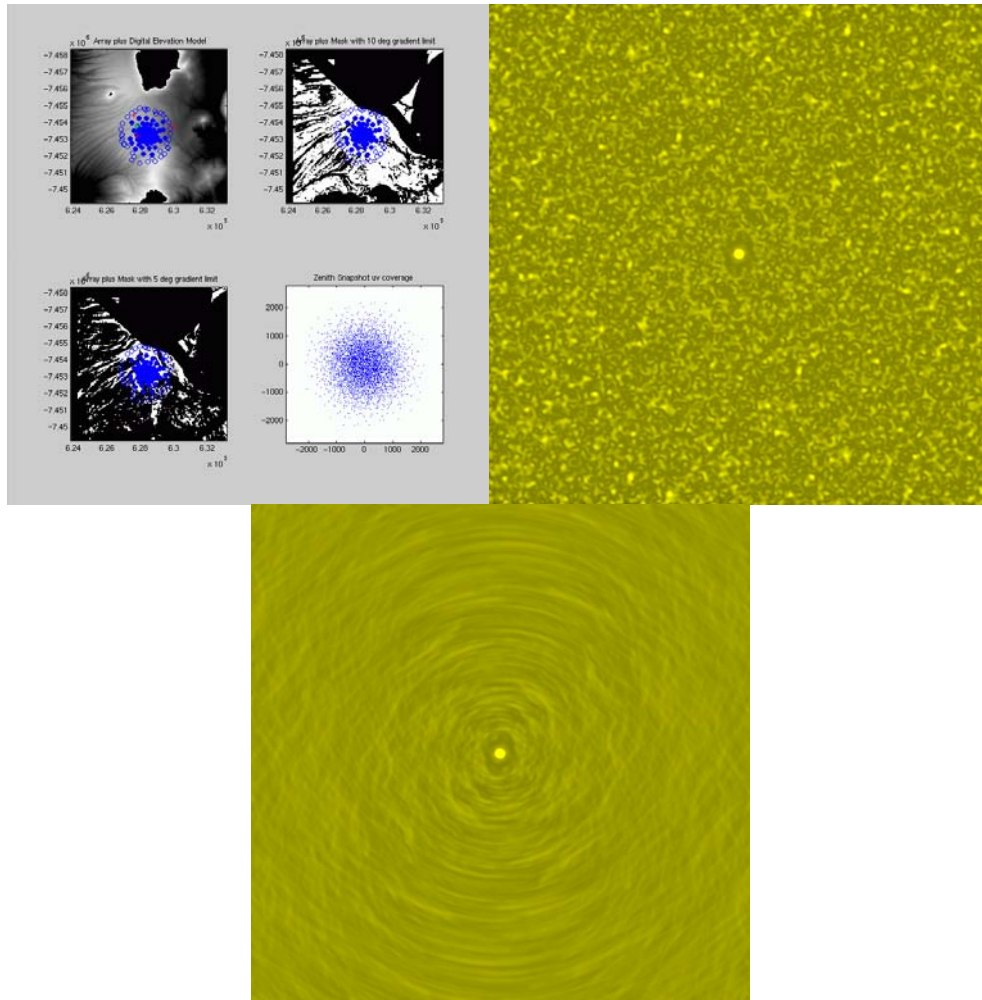


Fig 2.(left panel) Pad distribution superimposed onto terrain and uv coverage for B-array equivalent. (Middle panel) zenith snapshot dirty beam. The plotted grayscale ranges between -5% and +10%. The peaks sidelobe between radii of 1 and 22 beams is 0.0456. (Right panel) Long track dirty beam for a dec=-23 sources observed +/-2hrs from transit. Note all antenna weights assumed equal and image is naturally weighted. The peak sidelobe within 20 beams is 0.0215.

3.3 B/C-Hybrid Array:

For observing Northern hemisphere and far Southern sources it is useful to have 'hybrid' arrays which are extended in the North-South direction. Such arrays are possible in zoom designs simply by changing the order in which antennas are moved. Take as concrete example a zoom array which is being operated as a set of fixed arrays, then reconfiguring from B to C array takes a total of 32 antenna moves. We could move between B and C array keeping circular symmetry

all the time or alternatively we could form an hybrid array by choosing to move the Easternmost and Westernmost antennas of B array in first. If we chose this second option after approximately 16 antenna moves the array would be in a B/C hybrid, extended in the North-South direction. After finishing observing in the hybrid we now move in the northernmost and southernmost antennas; after another 16 moves the circularly symmetric C-array equivalent is reached. Note that whether we chose to go via a hybrid array or not the total number of antenna moves is the same.

In the case of a continuously evolving array rather than one with conventional 'burst' reconfiguration there are two options. One could keep to a similar scheme, of moving between circular and elliptical arrays but gradually moving antennas one or two at a time. Alternatively one could move out through the arrays sizes keeping circular symmetry and then go backward from the largest to the smallest array but now occupying pads always within an elliptical area.

Figure 3a shows an example of a zoom B/C hybrid array. The projected snapshot uv coverage for a declination +30 degree source is shown. Figure 3b shows the main lobe of the snapshot and long track (4hr) beams. At the half power level the extension in the N-S direction is only 1.15 and 1.10 respectively. Fig 3c shows a greyscale of the snapshot and long track beams. There are no significant N-S sidelobes although there is N-S 'apron' caused by the foreshortening in the N-S direction of the shortest baselines in the array.

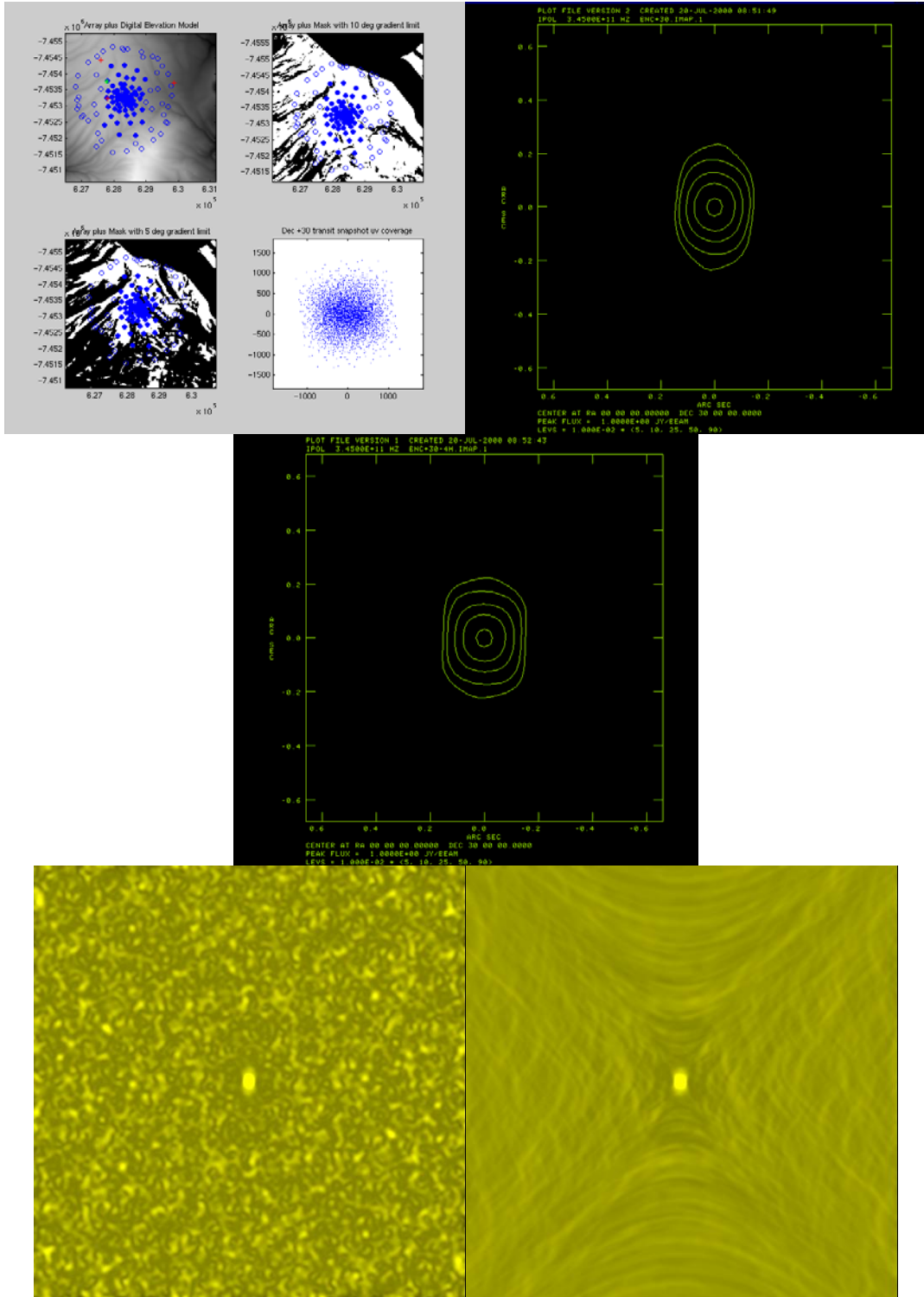


Fig 3 (Top Left) Antenna distribution superimposed onto terrain and the snapshot uv coverage for a transiting Dec +30 source observed with B/C hybrid arrays. (Top Middle) Contour representation of the snapshot main beam observing a dec=+30 source at transit. The fitted beam

FWHM is 178 x 153 mas. At the 50% contour the ratio of NS to EW dimension is 1.15. (Top Right) Long track dirty beam for a dec=+30 sources observed +/-2hrs from transit. The fitted FWHM is 176 x 160mas. Note all antennas weights are assumed equal and image is naturally weighted. At the 50% contour the axial ratio is 1.10. (Bottom Left panel) Snapshot dirty beam for Dec +30 source observed at transit. The plotted grayscale ranges between -5% and +10%. The fitted beam FWHM is 178x153 mas. (Bottom Right panel) Long track dirty beam for a dec=+30 sources observed +/-2hrs from transit. Note all antennas weights assumed equal and image is naturally weighted. The fitted beam FWHM is 176 x 160 mas.

3.4 C-Array Equivalent :

The array distribution, baseline distribution and beams for the zoom array C-array equivalent are shown in Fig 4.

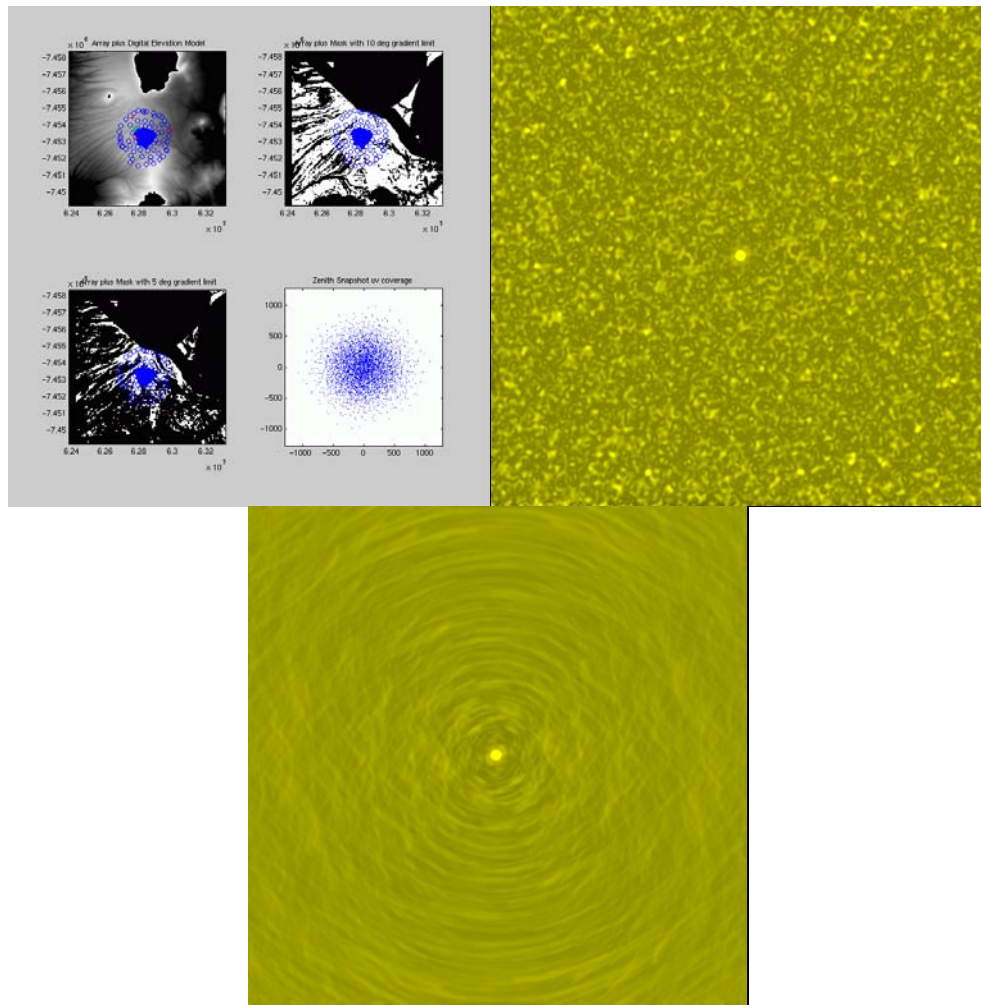


Fig 4. (Left panel) Pad distribution superimposed onto terrain and uv coverage for C-

array. (Middle panel) Zenith snapshot dirty beam. The plotted grayscale ranges between -5% and +10%. The peak sidelobe between radii of 1 and 22 beams is 0.0508. (Right panel) Long track dirty beam for a dec=-23 sources observed +/-2hrs from transit. Note all antennas weights assumed equal and image is naturally weighted. The peak sidelobe within 20 beams is 0.0276.

3.5 D-Array Equivalent :

The array distribution, baseline distribution and beams for the zoom array D-array equivalent are shown in Fig 5.

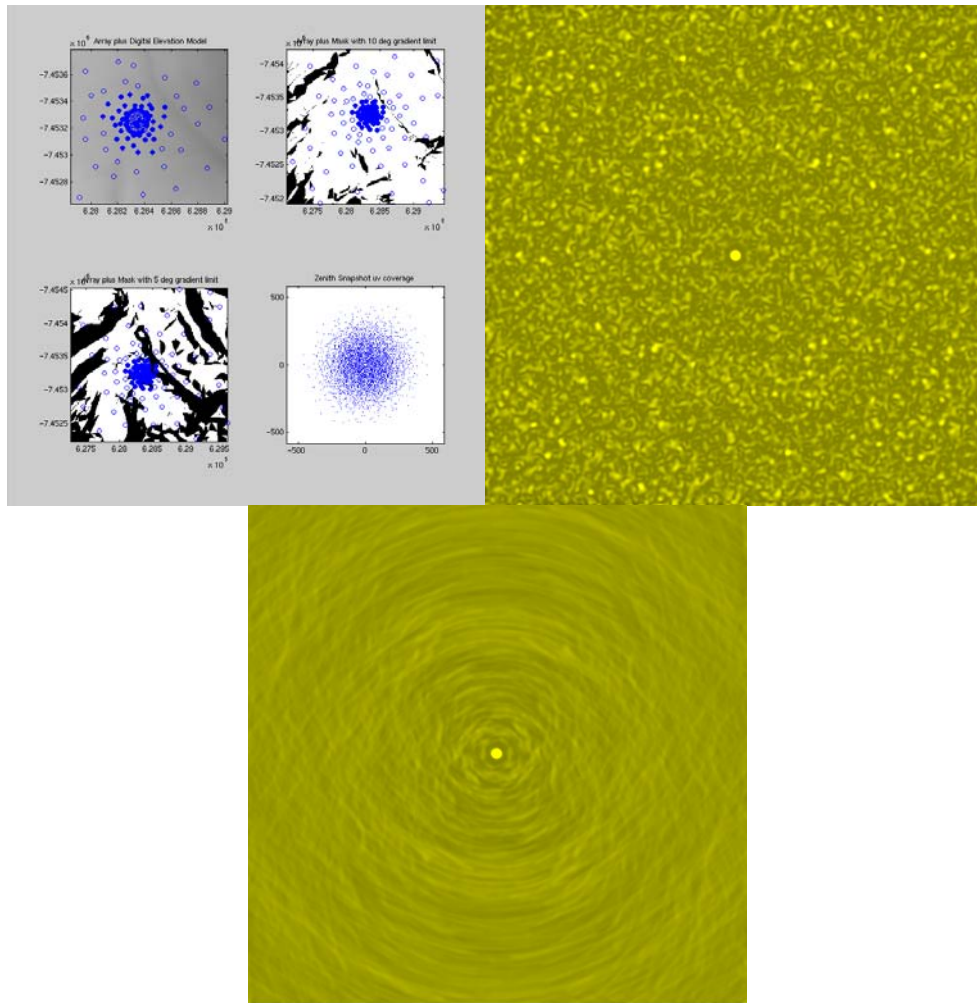


Fig 5. (Left panel) Pad distribution superimposed onto terrain and uv coverage for D-array. (Middle panel) Zenith snapshot dirty beam. The plotted grayscale ranges between -5% and +10%. (Right panel) Long track dirty beam for a dec=-23 sources observed +/-2hrs from transit. Note all antennas weights assumed equal and image is naturally weighted. The peak sidelobe within 20 beams is 0.0246.

3.6 E-Array Equivalent :

The array distribution, baseline distribution and beams for the zoom array E-array equivalent are shown in Fig 6. The zoom E-array is exactly the same as the E-array for the double ring strawperson arrays.

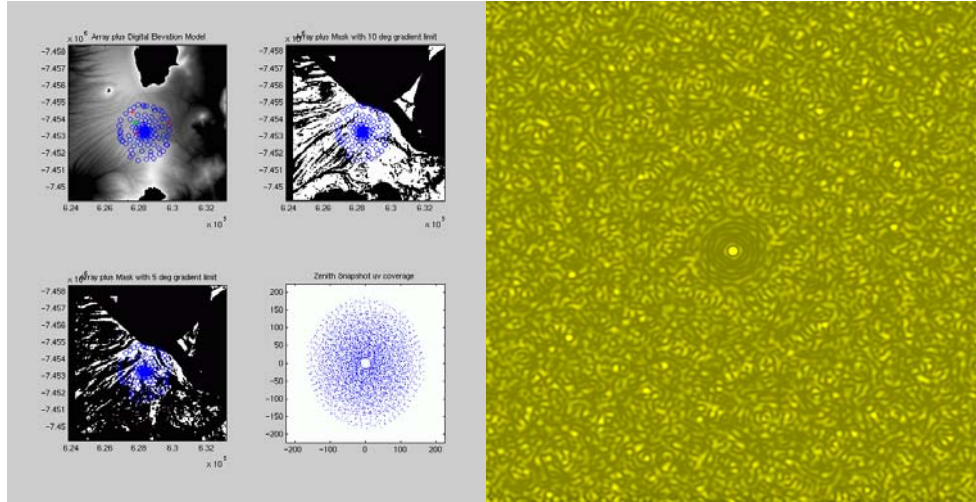


Fig 6. (Left panel) Pad distribution superimposed onto terrain and uv coverage. (right panel) Zenith snapshot dirty beam. The plotted grayscale ranges between -5% and +10%. NOTE No primary beam attenuation has been applied.

4. Comparisons with Double Ring Array: UV Coverages and Beams

In this section we compare the uv coverages and beams produced by the spiral zoom arrays with those produced by the strawperson double ring array (Yun and Kogan 2000). For the purpose of intercom parison we presented in Section 3 the uv coverages and beams for zoom configurations which were approximately equivalent in resolution to the A,B,C,D and E double ring arrays. It is impossible however to exactly match the resolutions and these slight differences should be taken into account when comparing results. The table below gives FWHM and PA of the beam fitted by IMAGR for a zenith snapshot observation. The frequency is assumed to be 345GHz.

Array Zoom	Ring						Min	Max	Ratio	Median	Mean	Rms
	Size	Min	Max	Ratio	Median	Mean						
A	79	3307	41	1595	1646	1277	87	3324	38	1581	1524	1230
B	32	2327	72	796	840	6687	35	1653	47	756	788	614
C	15	1068	71	345	365	293	15	868	57	339	380	296
D	15	489	33	168	178	140	15	420	28	170	179	139

Table 1. Baseline properties of zoom and ring arrays. All dimensions are in metres.

Array	Zoom			Ring		
	Size	Maj (mas)	Min (mas) PA (deg)	Maj (mas)	Min (mas) PA (deg)	PA (deg)
A	51.9	49.3	73	54.6	51.0	88
B	102.6	97.7	62	110.4	101.6	89
C	235.1	225.3	-14	236.3	206.2	-89
D	476	464	-67	489	444	89
E	970	900	-89	970	900	-89

Table 2. Snapshot beam properties of the two arrays.

Note that in most cases the zoom array has a slightly smaller beam than the double ring, the exception being C-array where the minor axis of the zoom arrays beam is significantly larger than that for the ring array, giving a more circular beam than the dual ring design.

4.1 Snapshot UV density distribution

The figures below compare the snapshot uv coverages and uv point radial density of the zoom and spiral arrays superimposed. The first order result is that the uv density distributions are quite similar. This is contrary to the claim made by Min and Yun (2000), that the uv coverages of the zoom array design are very centrally condensed compared to the dual ring design. At most one could say that the uv distribution is moderately more condensed. It can argued that this moderately more condensed coverage is actually an advantage for a) imaging complex sources with large amounts of diffuse emission and b) from the point of view of reducing the effects of residual atmospheric phase errors (see Section 5.9).

Given the different philosophies and starting points adopted for the two array designs the similarity of the uv density distributions is remarkable. This result shows that if we wish to have arrays which share about 50 percent of the pads between configurations different in resolution by factors of about 2 then a quite condensed uv point distribution is virtually inevitable. Since a high degree of pad sharing is required for operational reasons this means practical considerations force us to have a somewhat condensed uv coverages. This is irrespective of the arguments about whether a more uniform or a more tapered distribution is better from a image quality point of view (see Conway 2000b).

Despite the first order similarity in uv point radial distribution there are some differences. We have already noted that the uv radial distributions is slightly more condensed. Secondly for the zoom array the uv distribution is smoother and finally it extends to somewhat larger uv radius than the dual ring array. The larger maximum baseline for the zoom is a consequence of being more condensed, two arrays with the same resolution must have the same rms baseline length, if an array has a dense core of uv points it must also have outliers to compensate. Considering the question of uniformity the double ring array shows signs of steps in the uv point density, corresponding to its 'wedding cake' like uv coverage (see Fig 8 bottom row). These steps arise because the in-built scales of the array. The spiral array design is self-similar, has no special scales and therefore has a smooth uv point density distribution.

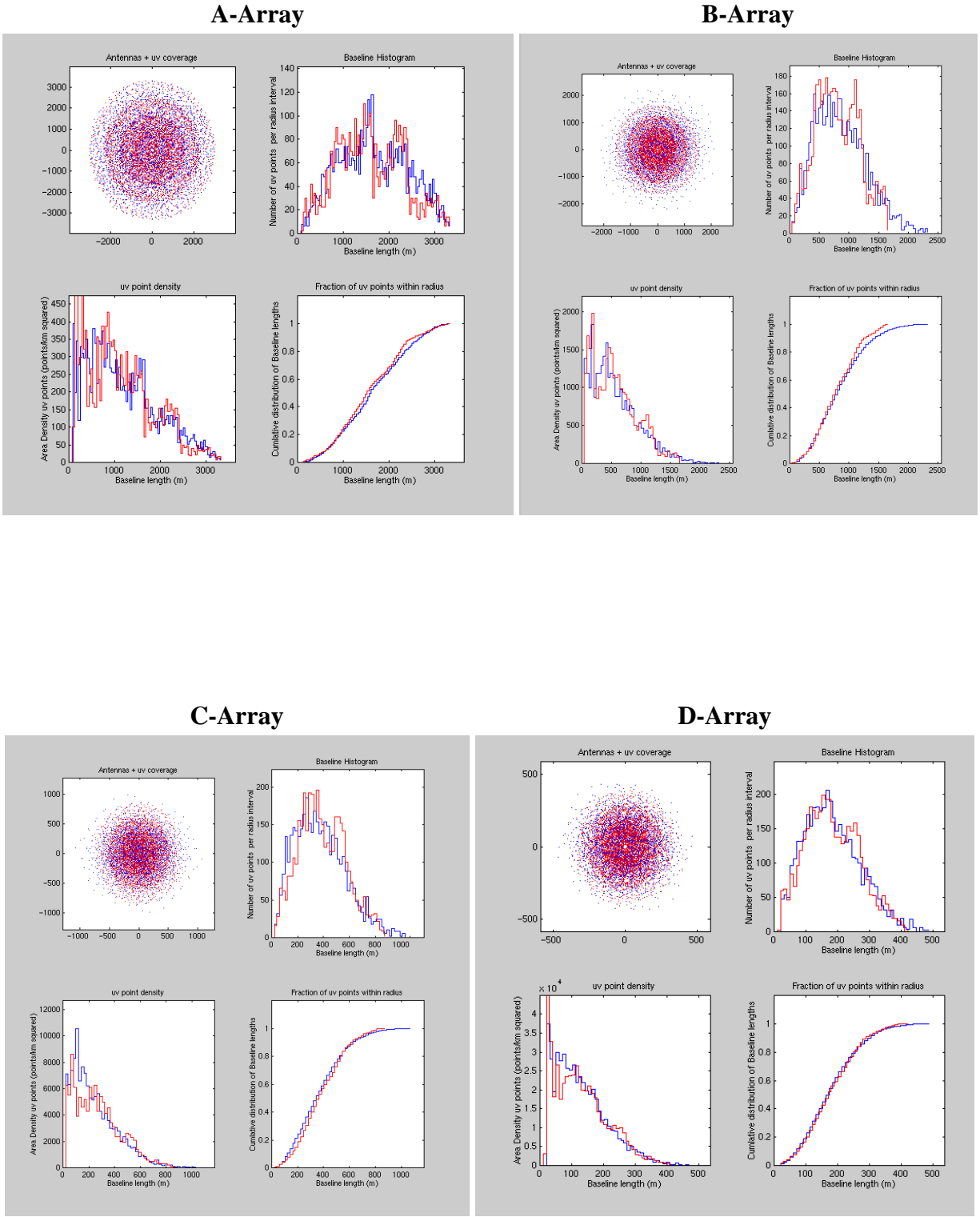


Fig 7. Plots showing radial uv density distributions for ring and zoom spiral arrays for each of the arrays A,B,C,D. The data for the zoom array is plotted in blue, while that for the double ring is plotted in red.

We consider now the larger maximum baseline for the zoom array; the ratio of largest baseline lengths between spiral and ring is 1.0, 1.16, 1.23, 1.41 and 1.00, in E,D,C,B and A arrays respectively. We note first that part of the reason for this larger extent is that the arrays are not exactly matched in resolution. As shown in Table 2 for most configurations the zoom array has slightly higher resolution, for instance in B-array the beam FWHM is 5% smaller. Secondly the fraction of the uv points in the spiral which lie beyond the largest baseline of the ring are in all cases small (despite the fact that the eye picks them up because they are at the edge of the uv coverage). For D and C arrays they comprise 2%-3% of the total, while for B-array they comprise 5% of the total.

Note that the median and rms baseline lengths for spiral and ring arrays of the same resolution are very similar. It can be shown that for arrays matched in resolution the rms baseline length must in fact always be the same. Having a wide range of baseline lengths has advantages in imaging for attempting modest super-resolution and giving overlap in baselines between arrays for combined array imaging. However, it might be imagined that configurations with longer baselines have the disadvantage that they have more phase noise. In fact it can be shown (see section 5.9) that for two arrays with the same resolution (and hence the same rms baseline length) that even in the worst case when observing a point source in the steep part of the Kolmogorov turbulence spectrum (rms phase proportional to $b^{5/6}$ where b is baseline length) -- phase errors of the two arrays must be virtually the same.

For baselines which are longer than the thickness of the turbulent layer the turbulence becomes 2 dimensional and the rms phase proportional to $b^{1/3}$; then in fact between two arrays with similar resolution the one with longer baselines will actually have lower integrated phase noise. This seeming paradox comes about because in order to have the same resolution the array with the biggest baselines must also have more short baselines (in order to give the same rms baseline length). These short baselines lie below the inner scale cutoff where phase errors rapidly decrease with decreasing b , and so the array has lower phase noise overall. Similarly when observing resolved sources the effect of the reducing uv amplitude with uv distance means that the phase noise contribution from the inner part of the uv plane dominates, which again for two arrays with similar resolution favours the slightly more condensed array.

4.2 Snapshot UV coverages and Dirty Beams

Below are plotted the zenith uv coverages and zenith dirty beams (assuming natural weight) in each array for the two styles of array. The uv plots for the ring arrays show the 'wedding cake' effect, i.e. tiers of different uv density superimposed. The effect of the corresponding dirty beam is to add systematic ring-like near-in sidelobes which are absent in the zoom spiral case. In all of the snapshot beams the peak sidelobe within 20 beams is about 5%, in the case of the zoom array this usually occurs at an isolated peak distant from the main lobe. In the case of the dual ring array it often occurs in the near-in sidelobe.

A-Array

B-Array

C-Array

D-Array

E-Array

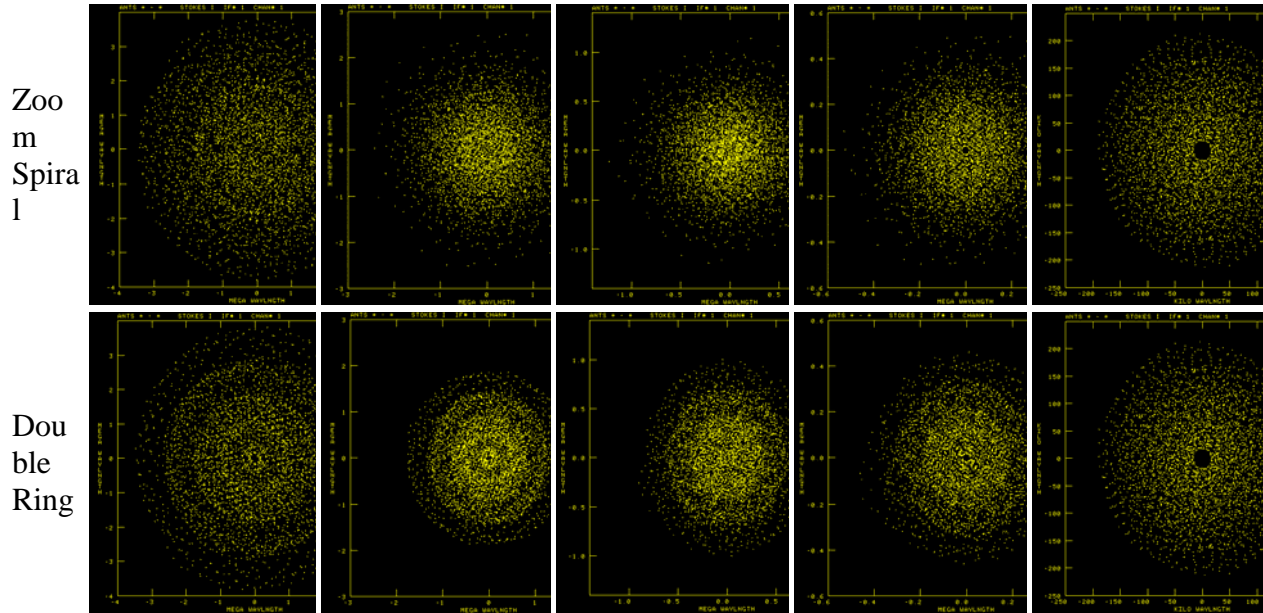


Fig 8. Zenith snapshot uv coverages for zoom arrays and the double ring arrays.

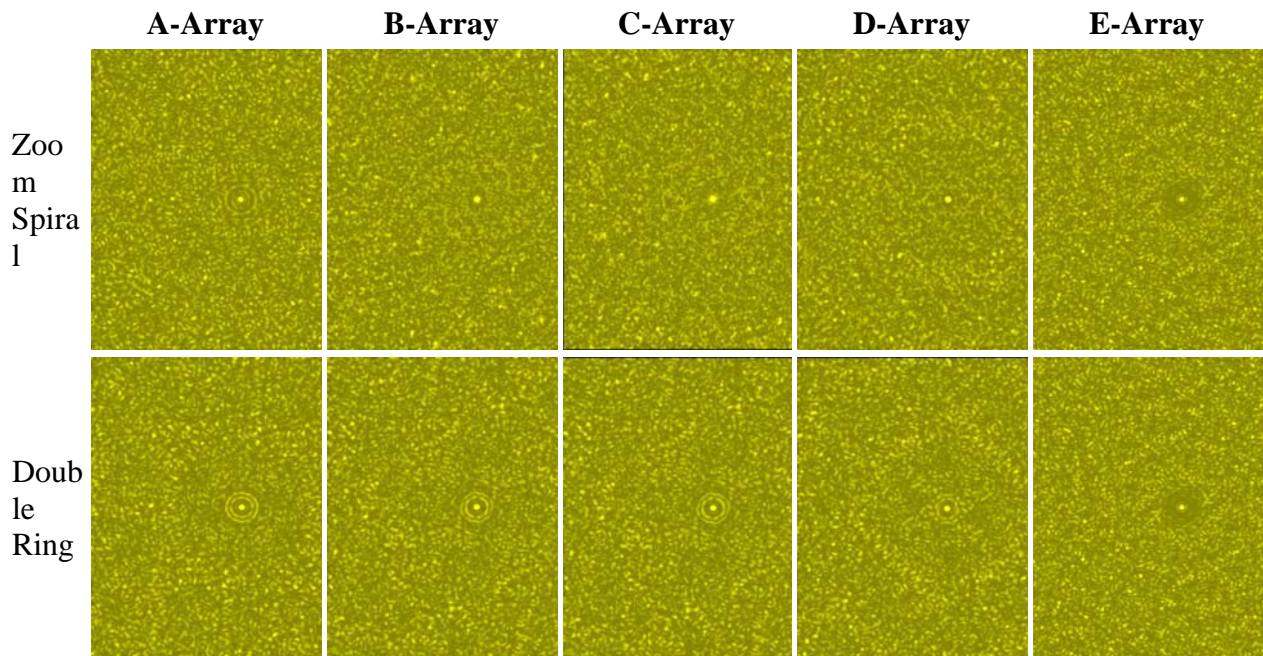


Fig 9. Zenith snapshot beams. Top row, room spiral. Bottom row double ring designs. From left to right beams for arrays A-E or equivalents are shown The plotted grayscale ranges between -5% and +10%.

4.3 Long track uv densities

Radial uv density distributions for long tracks of modest length (e.g 4 - 6hrs) are only slightly more centrally condensed than those for snapshots shown in Fig 7. The only effect which causes extra central condensation for long tracks is the foreshortening of the baseline as the source goes to lower elevation. For a millimetre array this is usually a large sensitivity penalty in observing a source at elevations at less than (say) half the maximum elevation, hence the effects of foreshortening are modest. To see that foreshortening is the only effect consider an array at the South Pole consisting of two rings in the uv plane, observing a source at the South celestial pole. It can be seen that the density of uv points in the two rings is always the same irrespective of whether a snapshot or long track is observed.

The plots below show the uv coverages for a 4hour long B-array track for a declination -23 source. This configuration size was chosen because it is the one which is most different between the two styles of array. The left hand plot shown below is for the zoom array and the right hand plot for the ring array. The red circle shown marked in both plots has a radius equal to the longest baseline of the ring array. Although the eye is drawn to the spiral tracks which lie beyond the outer circle relatively few uv points (about 3%) actually lie beyond the bounding circle. Despite the uv points beyond the outer boundary for this 4 hour track the fraction of filled cells within the circle is larger for the spiral than the double ring array. This effect arises because for the latter array a significant number of uv-cells at radii of 700m or 1200m are multiply sampled.

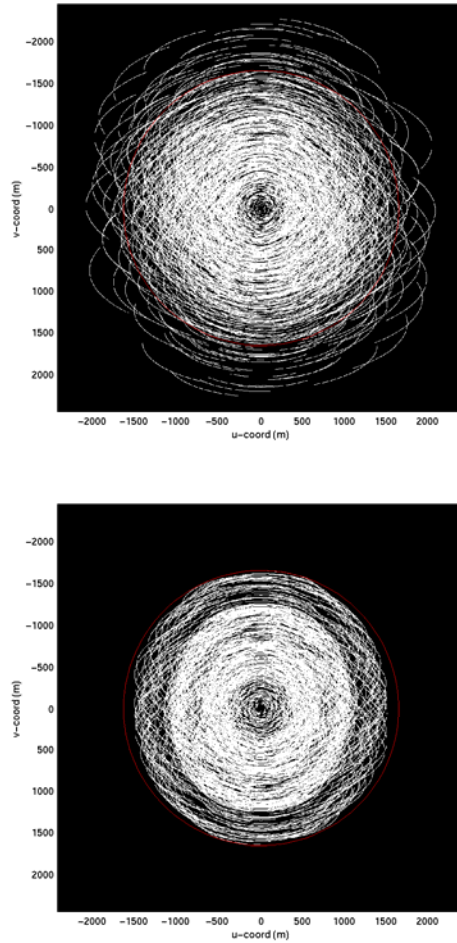


Fig 10. Long track uv coverages for a declination -23 sources observing +/-2 hrs across transit. Left - for the zoom spiral array. Right -for the double ring array. The red circle marked in both uv coverages has radius equal to the longest baseline of the ring array.

The plot below shows the fraction of filled uv grid cells sampled within a circle whose radius is set by the longest ring array baseline. For snapshots, the degree of is always slightly less for the spiral than for the ring array because about 2% - 5% of the uv points from the spiral have baseline lengths which exceed the longest ring array baseline. However as the integration time is increased for most arrays the sampling fraction becomes larger for the spiral than the ring array. The reason for this is that the coverage within the circle is more evenly spread for the spiral than for dual ring array, where the uv coverage it is 'stepped'. This causes, in long tracks there to be significantly more double sampled uv cells in the case of the ring giving a slightly lower uv cell occupancy. The exception to this behaviour is C-array. The difference probably arises because the resolution of the C-array equivalent spiral array is somewhat different from that of the C-array ring (see Table 2).

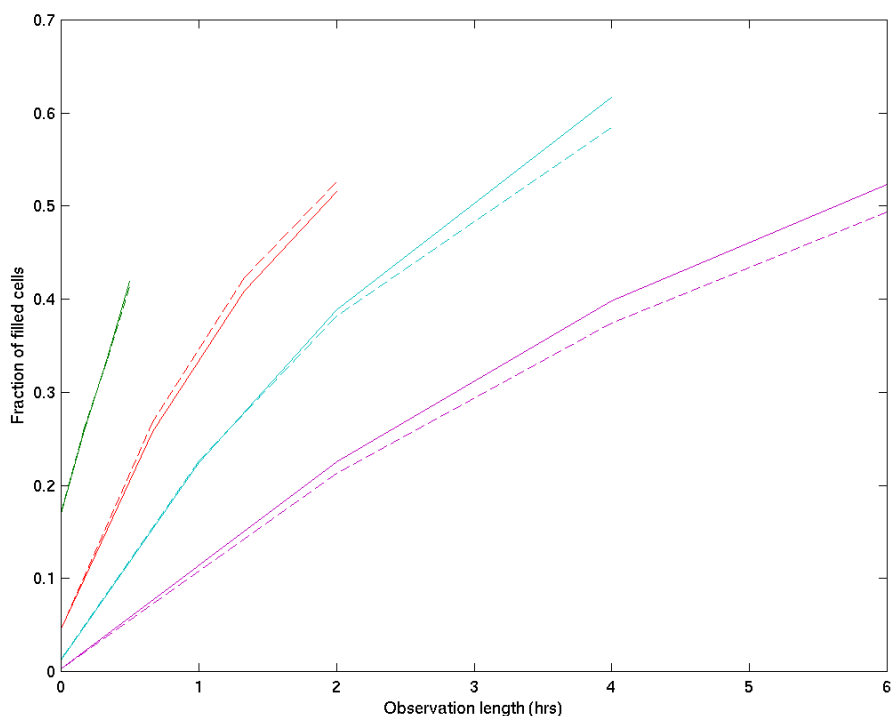


Fig 11. Fraction of uv cells occupied within circle equal in radius to the largest double ring baseline as a function of length of observation. A uv cell has an area equal to that of single antenna and the declination is assumed to be -23 degrees. The solid lines are for the zoom spiral array and dashed lines for the ring array. Purple is for A-array. Light blue B-array, Red C-array and Green D-array.

Note that if we chose a larger circle within which to evaluate uv occupancy the ratio of filled cells between zoom and dual ring arrays would increase. Since the two arrays have the same resolution clearly uv cell occupancy should be evaluated within the same sized circle.

It might be wondered whether for the zoom spiral the uv points in the very unevenly sampled part of the uv plane beyond the circle contribute significant high spatial frequency sidelobes. To investigate this we evaluated the contribution to the sidelobes from points in the spiral uv coverage which lie beyond the maximum baseline of the dual ring (simply by using UVRANGE in IMAGR to not include baselines smaller than UVCUT and rescaling the beam amplitude for the number of uv points involved). The relative contribution is shown in the figure below. The ring like near-in sidelobes are an artifact of the sharp cutoff applied in the uv plane - in a sense when computing the full dirty beam they are cancelled out by rings due to a sharply cutoff uv coverage from 0 to UVCUT which will have opposite sign. What is most significant is the level of the far sidelobes. In all cases they are less than 1% and are overwhelmed by sidelobes produced by the rest of the uv coverage. This test demonstrates that the outer uv points of the uv coverage do not give rise to significant sidelobes. This results should not be surprising; at maximum for long tracks only 3% of the points lie beyond UVCUT, and the far sidelobes are a coherent sum of the these uv points after rotating by a phasor which depend on the uv and xy

coordinates in the beam.

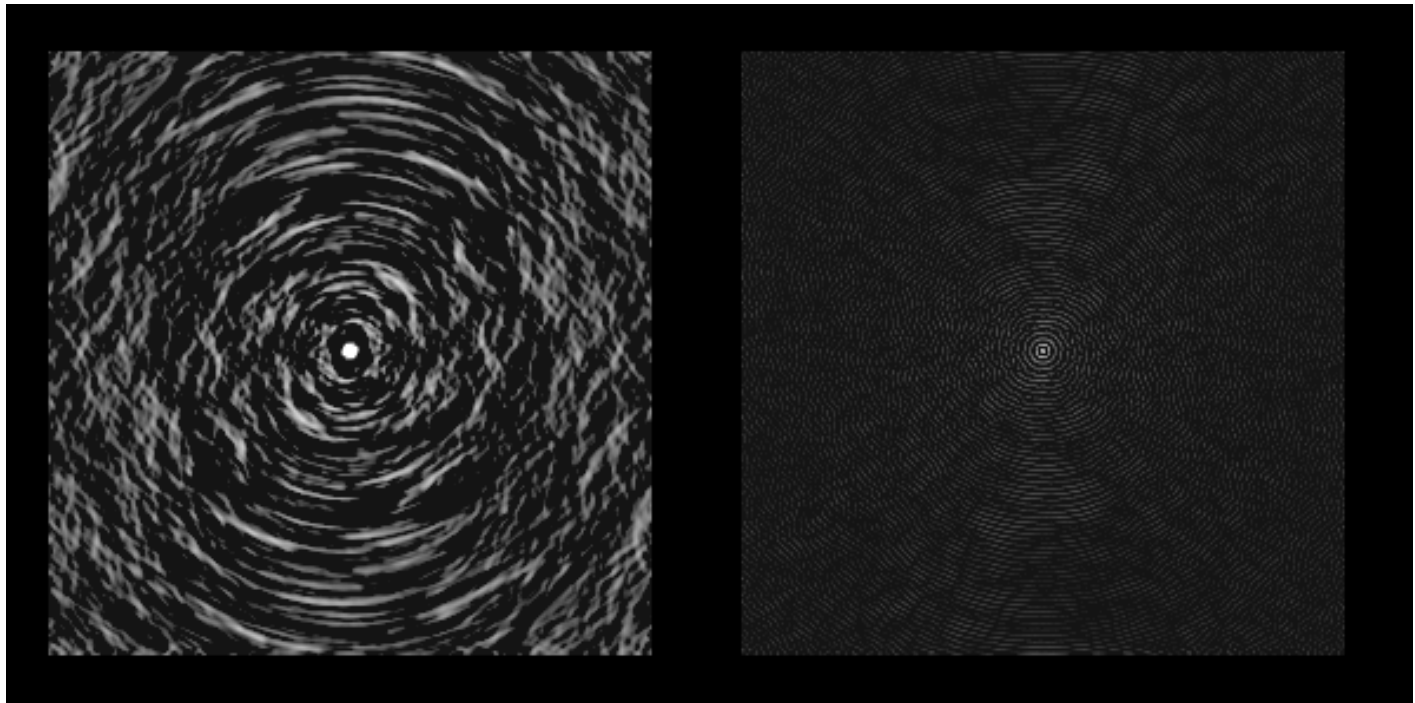


Fig 12. Left: Plot of the 4 hour B-array zoom spiral beam for a declination -23 source. Plotted between 0 and 3%. Right: Contribution to the dirty beam from the 3.9% of uv points which lie beyond the outer radius of the dual ring uv coverage, also plotted in the range 0 to 3%. The rings in the centre are an artifact of taking a sharp uv cutoff. The largest far sidelobe contributed by the outer uv points is 0.5%

4.4 Long track dirty beams

Below we compare the long track dirty beams for the zoom spiral and dual ring arrays. The main difference between them is that the latter has ring-like near-in sidelobes which the zoom spiral does not have. This causes a significant difference in peak sidelobes with 20 beams between the two arrays (see Table 3). On average the peak sidelobes of the zoom array are only 59% of the peak sidelobes for the dual ring. In addition the peak zoom array sidelobe occurs on a distant peak whereas the peak sidelobe for the ring array occurs a part of a coherent structure with many adjacent parts of the beam having almost the same value. The reason for the much larger near-in sidelobes in the case of the dual ring is the 'stepped' or 'wedding cake' nature of the uv coverage, while the uv coverage density distribution for the spiral is close to gaussian for all arrays other than A. Another useful way to look at the long track dirty beam is as a superposition of rotated and EW-stretched snapshot dirty beams. We can therefore see that although distant

sidelobes are decreased in going from snapshots to long tracks near-in sidelobes will be hardly decreased at all.

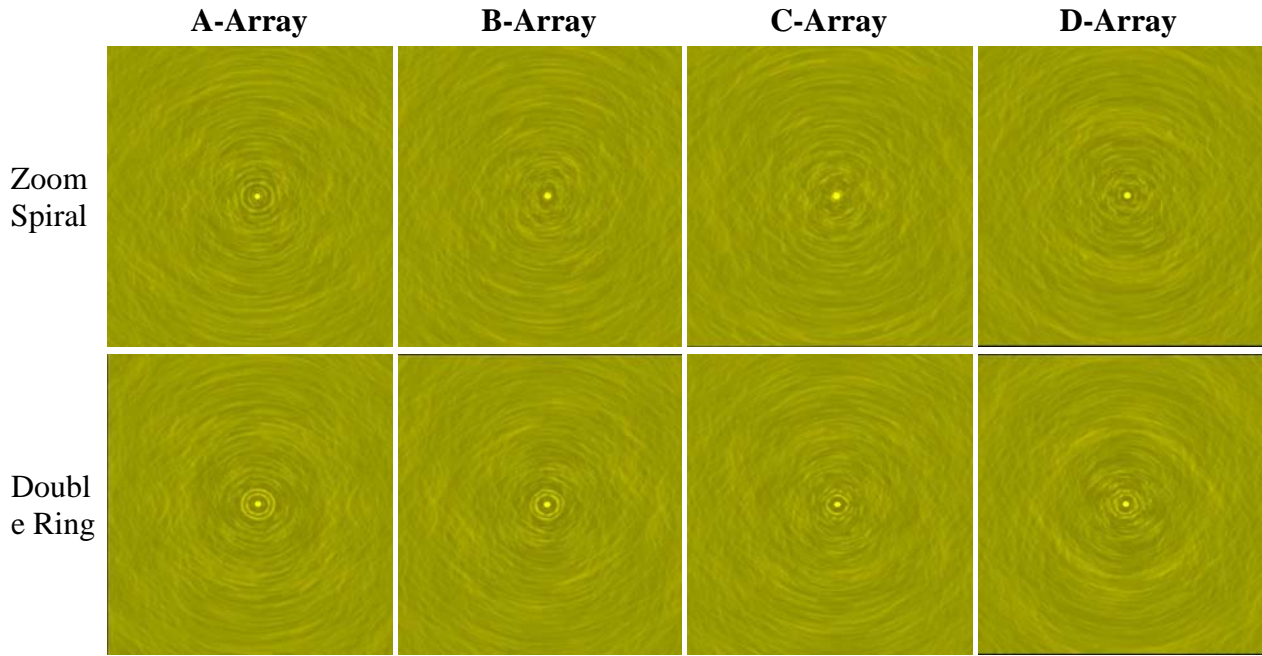


Fig 13. Long track (4hr) beams for a source at declination -23 degree, Top row, zoom spiral. Bottom row double ring designs. From left to right beams for arrays A-E or equivalents are shown The plotted grayscale ranges between -5% and +10%.

Array	Zoom	Ring	Ratio Zoom/Ring
A	0.0259	0.0427	0.60
B	0.0215	0.0385	0.55
C	0.0276	0.0469	0.58
D	0.0246	0.0385	0.63

Table 2. Peak sidelobes within a radius of 20 beam FWHMs for a 4 hour long synthesis of a declination -23 deg source, for the zoom and ring arrays respectively.

Below we show North-South slices through the dirty beams for the spiral and double ring arrays respectively.

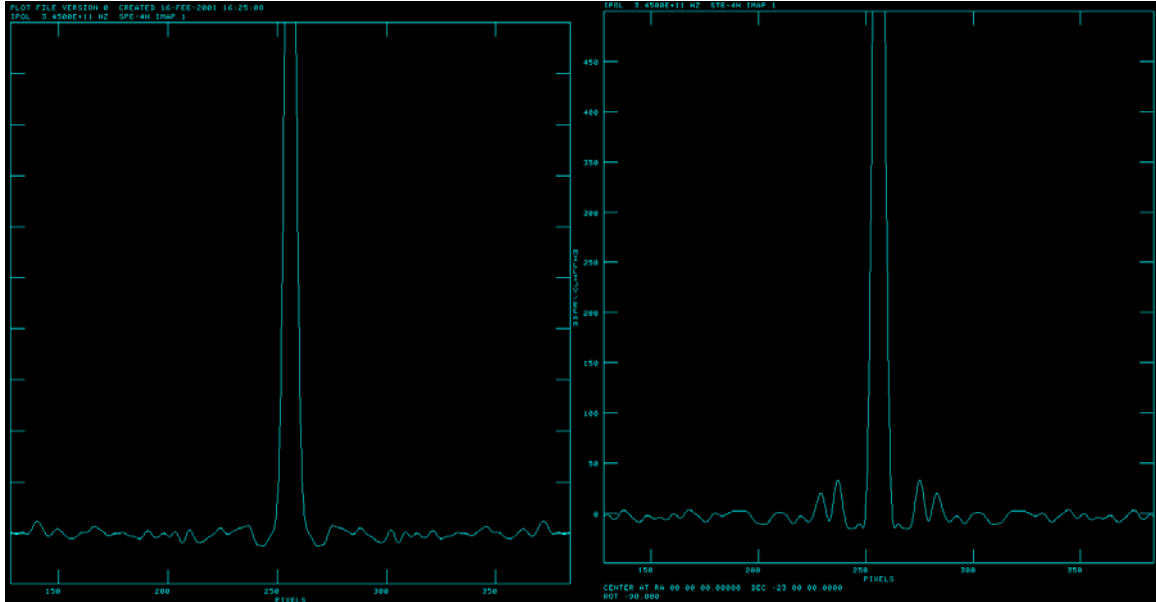


Fig 14 Left: A North-South slice through the B-array zoom spiral dirty beam. Right: A North-South slice through the B-array dual ring dirty beam.

4.5 Imaging Simulations

Both the ring and zoom arrays have been tested imaging a series of test images. The results of these CLEAN simulations can be found at [Heddles Simulation Page](#). Although in some cases the ring strawperson gives better reconstruction, in general the quality of the zoom array constructions are slightly better especially for long tracks. Usually at given brightness level in image the rms reconstruction errors are about a factor of 1.5 to 2 less. For B-array in particular the fidelity index metric in some cases gives a different result; implying a few (100 pixels is 4 beams) regions of very high fidelity index. It is unclear why this is difference between the the two methods of measuring image quality. Possibly when one adds both errors at a bright point to bowl like negative errors the value of the parameter (model/error) can have fortuitously large values at a few isolated points.

5. Comparisons with Double Ring Array: Operational and other considerations

In this section we consider other aspects of array design other than uv coverage and beam which can be considered operational or practical matters; and compare the zoom and dual ring array concepts for the intermediate configurations.

5.1 Array Flexibility

One of the most attractive features of the zoom array is that it is a very flexible design. In this memo we have concentrated on configurations of the spiral array in five nominal configurations which match in resolution configurations offered by the dual ring arrays. Note that this has been done to facilitate inter-comparisons between the two array styles; it does not imply that the array is restricted to these configurations.

The zoom array could in contrast to the the dual ring instead operate at say three fixed resolutions or seven, or whatever, with the choice of resolution being made after construction in response to the types of science that are popular in the 2010s or 2020s. For instance if line ratio imaging between particular molecular transitions became popular that could easily be accommodated. Note that the total number of antenna moves that must be made to accommodate different numbers of configurations is constant. Antennas are always moved from the outside pads to the inside pads and after making 126 antenna moves we will have moved all antennas from the largest to the most compact configuration. All that changes when we go to a smaller or larger number of configurations is whether antennas are moved in short of long 'bursts'.

At one extreme the zoom array also allows the possibility of gradually and smoothly changing the resolution of the array by for instance moving three antennas every four days or so. This approach has certain astronomical advantages in that all resolutions are offered removing the need to lose sensitivity by tapering. This approach also has operational advantages in that a small crew can be employed continuously for antenna moves which can then all be accomplished in the morning before winds get high. The array should also be more resilient to delays in moving antennas due to weather . The astronomical efficiency and operational aspects are discussed in detail in Conway (2000) memo 283 and are further discussed in the section below.

The zoom array no matter whether operated in burst or continuous reconfiguration mode is more flexible in another sense as well. Essentially it just comprises as $1/r^2$ pad density distribution without any in-built scales. This allows a great flexibility in how the pads are populated in any given configuration. This population scheme can be changed in response to observing experience just like the case of the VLA where C-array was recently altered to allow more short spacings. The zoom array probably gives more flexibility in this regard than the dual ring in which all antennas must be placed on a limited number of concentric rings.

5.2 Operational Issues

Both the zoom spiral and dual ring arrays have virtually the same number of antenna pads (195 for the spiral and 192 for the ring) and require virtually the same number of moves to go through all configurations smaller than 3km (126 for the zoom spiral and 128 for the dual ring). What potentially is different is the order and tempo of how the antennas are moved during a reconfiguration cycle. When considering the operation of the zoom array it is useful to consider two possible operation plans namely 'burst' and 'continuous'.

'Burst' reconfiguration - In this mode the zoom operates just like the dual ring array with fast reconfiguration between a set of fixed resolution arrays. We will we assume that just like the strawperson dual ring design the zoom operates in 5 array size smaller than 3km (although of course the number can be varied for the zoom). In this case every year we can spend two periods of 4 weeks in each array size (A,B,C,D,E). It could take perhaps 4 days to reconfigure between configurations (assuming we move 8 antennas per day) North-South elongated 'hybrid' configurations can be accommodated (see Section 3.3) in two possible ways. If only a small amount of hybrid time was requested by astronomers we would simply move the eastern and western most antennas first during the 4 day move period and slot observations in once antennas

had calibrated baselines. If much more hybrid time was requested we could break the reconfiguration into two halves. In the first half the 16 easternmost and westernmost antennas would be moved, taking two days to reconfigure, giving the North-South hybrid. Perhaps a week would be spent in the hybrid configuration plus two more days reconfiguring. In this mode of course only 3 weeks could be spent in the the full configurations (A,B,C,D and E). In addition to all of this there would be one period per year of perhaps 4 weeks in the 12km configuration.

'Continuous' reconfiguration - In this mode the array is reconfigured slowly but almost continuously. Because of the need to calibrate antenna pointing before a moved antenna can join the array (and the need to determine sub-wavelength accuracy baselines - although this can in principle be partly done later and the corrections added to the correlated data) it is probably not efficient to move less than 3 or 4 antennas at once. In Conway 2000a (memo 283) a scheme was proposed to move 3 antennas twice a week, on Mondays and Thursdays. On average then a complete cycle through all the configurations smaller than 3km (126 moves) would take 21 weeks. Two full cycles could be accommodated per year, adding 2 extra weeks twice a year 'stopped' in each of A and E arrays. Finally there would 6 weeks per year in the 12km array (including move time) scheduled once a year. The overall cycle structure is indicated in the figure below. During the continuously reconfiguring part of the cycle, the Monday and Thursday moves could for instance be accommodated by 3 transporters and three crews taking 1 - 2 hours to do the move, and all moves completed by 9am or 10am local time. A crew of 6 would be used for reconfiguration. On other days when not reconfiguring these personnel would be used for antenna maintenance. There would in the suggested cycling scheme be three long moves per year when all transporters (5?) and all available staff used to move antennas as quickly as possible. These 'long moves' could comprise the moves to and from the 12km array and from the E to A array.

During the main periods of continuous reconfiguration there will be occasional Mondays and Thursdays when a reconfiguration is not possible due to high winds or snow. In this case the reconfiguration can be attempted on one of the two or three following days that otherwise would be allocated to antenna and receiver maintenance. If these days were also effected by weather we could try to attempt two configurations per crew on the next scheduled reconfiguration day and so on. In the scheme suggested below the array would be reconfigured inwards starting with A array and shrinking the array to E array. This means that if a reconfiguration was missed the scheduled astronomical observation would go ahead, but with a resolution that is 7% larger than originally scheduled. By gaussian tapering the data the desired resolution can be recovered with a loss of only 2% in sensitivity (see Conway 2000a, memo 283).

Hybrid arrays can be incorporated into continuous reconfiguration in two possible ways. In the first method for 5 reconfiguration days (2.5 weeks) the Eastern most and Western most antennas are preferentially moved inward and then for the next 5 reconfiguration days (2.5 weeks) the Northernmost and Southernmost antennas are moved. For most of the 5 week period the beam would be fairly round (and a perfectly round beam can be recovered with little sensitivity loss by suitable tapering), but in the middle of this period the array would be extended North-South with good uv coverage and near circular beams for sources as far north as declination 30 degrees. In the second method we could move inwards through the arrays keeping circular symmetry twice a year and outward through the configurations once per year this time filling antenna pads within

an elliptical area.

A possible phasing of the reconfiguration cycle with respect to season is also given in the figure below (this is only a first suggestion). Amongst the issues to be considered in deciding the phasing is the desire for both high resolution (A) and compact (E) array observations to have the high phase stability, high opacity winter weather, and the operational desire to move to and from the 12km array during the least windy months (say November and December).

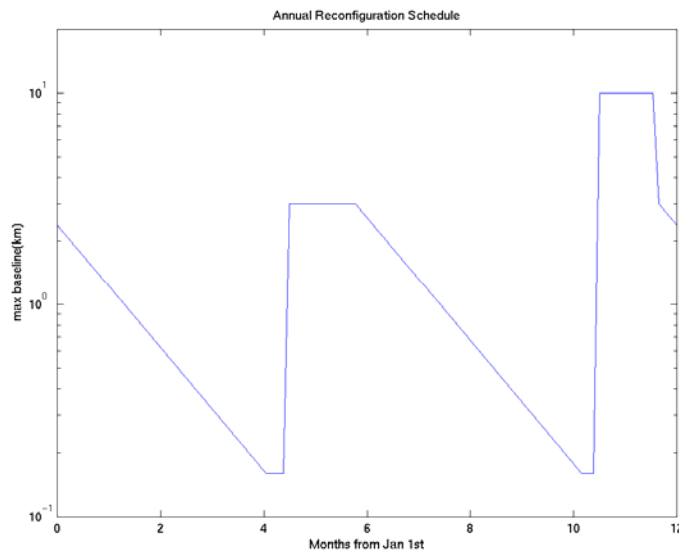


Fig 15. A possible reconfiguration scheme for ALMA using continuous reconfiguration. Click for higher resolution.

In comparing the operational aspects of running the zoom spiral with the dual ring strawperson we can distinguish between generic advantages inherent in the array geometry and the advantages of using continuous reconfiguration.

Generic Advantages One important difference between the two arrays is that however the zoom is reconfigured (either via conventional bursts or continuously) it is always left in a self-similar configuration - so the uv coverage is always smooth with a good beam pattern. This is in contrast to the dual ring array - if bad weather hits at the start or end of a 'burst' reconfiguration period then antennas can be left 'stranded' on either the inner or outer ring. The uv coverage of an array with only 2 or 3 antennas on the outer ring will not be particularly good and the data from these antennas will in practice often be deleted. Note that the wind limit for observing (at low frequency) is less than that for moving antennas. Consider also the scenario that reconfiguration starts in the morning but winds rise during the day and reconfiguration must be abandoned. The winds will die down again in the evening and observations can begin again, but it will be dangerous and undesirable to reconfigure during evening/nighttime. The array will then have as much as 16 hours of observing time (often of excellent quality) in a non-optimum configuration.

Advantages of continuous reconfiguration Some of the advantages of continuous

reconfiguration, such as a permanently employed crew at the site, and the ability to do all reconfigurations early in the day before winds rise have already been mentioned. There are also astronomical advantages in that resolutions in different line transitions can be matched without losing sensitivity due to tapering. It can also be argued that continuous reconfiguration is more robust to weather related problems. In the case of conventional burst reconfiguration if a period of bad weather lasting say a week hits during the scheduled reconfiguration period the whole cycle of configurations can be effected. Instead of 4 weeks in the next configuration only 3 weeks will be possible, and a significant number of projects will have to be delayed six months or observed in configuration a factor of 2 different in resolution to that requested. More seriously the schedules of the personnel involved in reconfiguration have to be changed, and the whole large crew put 'on standby' until daytime weather is good again. It can of course be counter-argued that with continuous reconfiguration we are also virtually certain to lose some reconfiguration days due to weather also. However is surely best to share and dilute the risk rather than concentrating it into a few big moves. An analogy can be made that most of us choose to insure their car and have a 100% chance of losing \$500 per year rather than a 1% chance of losing \$50,000.

5.3 Hybrid Arrays

As shown in Section 3.3 the zoom array geometry can easily accommodate North-South elongated hybrid arrays for looking at far Northern or far Southern sources. The resulting uv coverages are smooth, the resulting dirty beams have no large sidelobes, and are close to circular for sources for declinations up to +30. Note that the total number of moves required to go through all array configurations stays the same whether or not one uses hybrid arrays or not.

Although an example was only shown for a B/C hybrid, similar hybrids are possible for all arrays. This includes the possibility of a D/E hybrid which is particularly useful because of the high degree of shadowing that occurs in E array for observations of far Northern or Southern sources. No comparable plots of beam shapes or uv coverages have yet been produced for the dual ring arrays to directly compare. For this design hybrid arrays would be produced by moving the Eastern or Western most antenna in the outer ring first. Since the ratio of radii of the rings is approximately 2 it is unclear whether the resulting uv coverage will be good.

5.4 Fitting the array into the Site.

In a recent memo Butler and Radford (2000, Memo 338) have identified a number of places which are suitable from the point of view of smoothness and flatness for placing the centre of the array. They have also investigated positions identified in the strawperson designs.

Note that the zoom array design described in this memo ('zoom2') has **exactly the same centre** as the strawperson dual ring array produced by Yun and Kogan (2000, memo 320). This was done deliberately to facilitate comparison between the two design styles, it did not necessarily imply that this was the best place to centre the array. In the memo of Butler and Radford the position which is discussed as 'spiral centre' in the position identified in the 'zoom1' design (Conway 2000c, memo 292), not the one used in this memo. In any case both centres were found to be less than optimum from a site point of view.

The site identified by Butler and Radford as 'Chanjnantor Best' is difficult to use for any design which has a high degree of pad sharing because it lies right at the edge of the 3km flat area at Chanjnantor. The second best site which is near the NRAO containers however is a possible candidate, since it lies halfway between the centre of the 3km flat area and its perimeter. Experiments with zoom arrays with an offset centres at this place show that relatively little distortion or 'squint' is introduced into the dirty beam and that the uv coverages remain quite good. A preliminary offset design will be presented very soon in a separate memo, (a preview of work in progress can be found at [Offset Zoom Array](#).)

For some reason there is a perception that it is harder to fit a zoom design into the site than a dual ring design, but this is not true. Considering non-offset concentric arrays it is clear that once the largest array size and the resolution step between rings is defined there are only two overall degrees of freedom (plus local distortion) in placing the array into the site, namely the x and y coordinates of the array centre. In contrast for a zoom spiral design the array can be rotated to avoid obstacles without changing the circular symmetry of the uv coverage. In addition one can choose either clockwise and counter-clockwise designs and can vary somewhat the pitch of the spiral arms to avoid obstacles.

5.5 Roads and Conduits.

A detailed road and conduit plan has not yet been made, however sketches suggest pads can be connected in the zoom array using 5 branch roads radiating from the centre, and curving to avoid quabradas, with additional 'twig' access roads to the pads. The pads on the outer ring would also be partly connected together where the terrain allows it. A sketch suggests a total road/conduit length for the smaller than 3km arrays of about 19km for the zoom. For the dual ring arrays connecting all the circles together takes 17.5km, plus two radial access roads adds another 3km, giving 20km. The total length of roads and conduits is likely in practice to be very similar for both styles of arrays.

5.6 Combined Array Imaging

For the most complex sources it is clear that data from several configurations must be combined to achieve the best imaging. This should cause no special problems for the zoom array. The uv density distribution of a single configuration is gaussian shaped (see Figure 7), with a flat top at intermediate to short baselines and then a hole in the centre of the uv plane which is approximately 1/40 or 1/50 of the longest baseline. The distribution differs significantly from the VLA which is not flat topped but is power law until a sharp cutoff at small baselines; this peaked uv density makes combining arrays more difficult.

To fill in the hole in the centre of a single configuration spiral uv coverage a snapshot in an array two or three sizes smaller should be added. For instance to B array could be added to D array observations. To obtain a smooth uv density distribution at the centre of the uv plane the integration time of the D array snapshot need only be $1/2.1^4$ or 1/20 that of the B-array; or 12 minutes in D array for a 4 hour long track in B-array. To make the inner parts of the combined uv density density smooth it may be necessary to re-weight the D-array data losing some

sensitivity but this loss is easily made up by integrating two or three times longer in D array. Finally after using them to cross amplitude calibrate the two configurations it might be desirable to delete the shorter baselines of B array, since the uv plane filling due to these baselines is much more ragged than the overlapping smooth uv coverage due to the smooth D array snapshot. Because a relatively small fraction of the B array uv data is effected (10% -20%) the loss in sensitivity due to doing this re-weighting will be small.

It is not envisioned that there will be any significant difference in combined configuration performance between dual ring and zoom spiral designs, because to first order the uv point density distributions are so similar.

5.7 Mosaicing

Testing the performance of the candidate designs in mosaicing mode has been limited to date by the lack of available software. Again given the similar uv density distributions of the two candidate array designs it would not be expected that there would be a large difference in performance. In particular both styles of array have exactly the same design for E-array. For D array both designs fully occupy the 150m diameter ring giving the same number of very short baselines going down to a fraction of an array diameter.

5.8 Pointing Errors

One of the factors that will limit the quality of ALMA Images at intermediate and high frequencies will be the effects of pointing errors. These have been simulated by Kogan(2000) (memo 317) and Morita (private communication). Again given the similar radial uv distributions we expect the zoom and ring arrays will have a similar response with respect to pointing errors.

It has been noted that pointing errors can limit the advantage of an array with better imaging performance. It should be noted however that the likely limitation in fidelity due to pointing errors is a strong function of both the source structure and the observing frequency. At 230GHz assuming a pointing error rms of 0.6" and using an image consisting of equally bright regions scattered over the primary beam Morita found that on-source fidelities for a spiral array were reduced from about 100 (with no pointing errors) to 75. Hence although significant the effects of pointing error were not dominant. The tested array still performed significantly better than another test array (a simple single ring array). The contribution of pointing to amplitude errors will scale quadratically with frequency for bright regions at the centre of the beam while it will be linear for regions near the half power point. For isolated sources with their brightest points in the centres of the beam and/or observations below 115GHz there will be many cases where pointing error effects are smaller than those due to uv coverage effects. Although the computing requirements are immense it is also possible that the antenna based pointing offsets can be solved for as part of the imaging process.

5.9 Phase Noise

In a separate memo we consider the phase noise effects in the image domain for two arrays with the same resolution but different degrees of central concentration. In the case that all baselines in

a configuration are smaller than the thickness of the turbulent layer (often 500m at the ALMA site, Robson 2001, Memo 345) then rms phase errors are proportional to $r^{5/6}$ where r is the baseline length, for longer baselines rms phase errors are instead proportional to $r^{1/3}$. We assume the worst case that we apply phase correction (e.g total power monitoring) and the corrected phase errors have the same dependence on baseline length but with the amplitude of the phase errors being scaled down. This would occur for instance if there were an error in the derived scaling factor between the atmospheric phase and the total power. In the case of observing a point source in the small baseline regime we show that phase error image errors are proportional to the $r^{10/6}$ moment of the array baseline length histogram. The resolution of an array depends on the second (r^2) moment of the same histogram, hence in this regime two arrays with the same resolution but different degrees of central concentration have virtually the same image phase errors (with a slight advantage to the more condensed array). If the source is resolved then the phase noise due to short baselines dominates more. These short baselines have smaller phase noise compared to longer ones; therefore out of two arrays with the same resolution the more concentrated one with more short baselines will have smaller phase noise. Similarly if we consider configurations in which many of the baselines are longer than the atmospheric turbulence thickness $r_{\{o\}}$ the more concentrated array again has lower phase noise errors even for a point source. We can see this because all baselines longer than $r_{\{o\}}$ contribute virtually the same phase noise but baselines with r less than $r_{\{o\}}$ have a rapidly decreasing phase noise contribution with r . Between two configurations with the same resolution, the more centrally concentrated one will therefore have less phase noise. The above arguments lead to a counter-intuitive result, that between two arrays with the same resolution the one which has a longer maximum baseline can have lower phase noise. The reason is that if an array has a small percentage of distant uv points then to give the same resolution it must also must have significantly more short baselines which more than compensate.

5.10 Tapering.

It is often useful to reduce the resolution of an array by increasing the weight of the short baselines. This procedure compared to natural weighting always increases the noise per beam; however the signal to noise to diffuse low brightness temperature emission can be increased by this procedure. Figure 9 of Conway 2000a (memo 283) shows how the loss in sensitivity in terms of increased mJy/beam changes as the array is gaussian weighted to give a larger beam. The noise only increases gradually with tapering, and reached an increase of factor of 1.13 once the beam is tapered to give 1.4 times larger beam size. Given their similar radial uv density distributions only minor differences are expected between zoom and ring array styles for loss of sensitivity as a function of tapering. However it is expected that the zoom array will be slightly more efficient since it is slightly more concentrated, as has been borne out by simulations.

5.11 Inverse Tapering and Super-resolution

To increase the resolution of existing arrays uniform weighting is often applied. This is a fairly crude procedure which looks at the local density of the uv coverage (i.e. uv points per uvcell) and weights inversely according to the occupancy. This procedure is very useful for the case of VLA data where it reduces the effects of the spikes in the uv coverage due to the intra-arm baselines. When applied to the fairly smooth radial uv coverages of the zoom and ring arrays it is

less successful (there is a sharp transition in weighting at a uv radius where the cell occupancy becomes greater than 2). For both array styles significantly increased sidelobe levels result. A more logical way to increase resolution is to instead apply global radial weighting methods which emphasise the longer baselines. Seeing the problem from constrained optimisation point of view it is possible to work out the optimal weighting as a function of uv radius for a given beam size (i.e. a fixed weighted mean square baseline length) which minimises sensitivity loss.

It is well known that in addition to applying uv re-weighting to increase resolution it is also possible to choose a somewhat smaller CLEAN restoring beam. CLEAN or other deconvolution algorithms extrapolate the uv data to larger uv radii than those measured. This extrapolation is always limited in quality and we convolve with a restoring beam to reduce its effect in the final map. In a sense the step of using the clean beam can be thought of as regularising the problem to answer the question of what the sky would look like if it was first convolved with a particular restoring beam before being observed. The Fourier transform of the CLEAN beam restored image certainly equals the uv coverage that would have been obtained from a hypothetical source which was convolved with the restoring beam before being observed. Seen in this way the choice of the size of a CLEAN beam can be seen as a fairly arbitrary step. No simulations have yet been performed comparing the performance of the two array styles with super-resolved CLEAN beams, but since the zoom spiral baselines extend to larger uv radius in a given configuration it is probable that the super-resolution performance of the zoom might be slightly better.

6. Summary

In this memo we have presented a strawperson zoom array design and compared its properties to the competing dual ring array design. We argue that compared to the competing array the zoom has a number of advantages.

1. Imaging Quality As discussed in Section 4 the peak dirty beam sidelobe level for snapshots is comparable for the two designs but for long tracks the zooms' sidelobe peak is 60% of the level for the ring. The radial uv distributions are smoother for the spiral with less clear holes. The uvcell filling factor is comparable with the spirals filling factor being slightly smaller for snapshots and slightly larger for long tracks. The present spiral designs have a wider range of baselines compared to the ring. CLEAN Imaging simulations appear to show a trend of somewhat higher dynamic range (by a factor of 2) for the spiral than the ring. Although pointing errors will eliminate differences in imaging quality in some cases; in other cases (e.g 115Ghz observations of isolated sources) imaging quality differences will remain an issue.

2. Flexibility The zoom is a very flexible array and can be operated in a wide number of different modes. It can be operated as a set of fixed configurations with the number and resolution of the configurations being adjustable. It also has the option of being run as a continuously reconfiguring array, which has certain operational and astronomical advantages. The mode of operation for the zoom can be changed easily after construction in response to changing scientific demands once the array is in operation. Finally there is more flexibility in the choice of pad occupation schemes than is the case for the dual ring.

3. Hybrid Arrays The zoom geometry has demonstrated excellent uv coverages and beams

when in North-South elongated hybrid arrays suitable for observing far North or far South sources. No extra pads need be built to accommodate a hybrid D/E configuration which is needed to avoid shadowing for observing Northern hemisphere sources. Unfortunately no similar hybrid configurations have yet been presented for the dual ring design to allow a direct comparison to be made.

4. No Stranded Antennas Whether operated in 'burst' or 'continuous' reconfiguration mode; after making an antenna move the array is always left in a self-similar pattern, all that changes is the resolution. In contrast for the dual ring if reconfiguration must be interrupted due to weather reasons there can be a few antennas 'stranded' on the outer ring, giving poor uv coverage, whose data would in practice often be deleted.

5. Lower Phase Noise In the case of observing point sources in the small array limit both array styles are expected to have the same image phase noise after doing total power phase correction. However for observations of resolved sources and/or observations with configurations with baselines longer than the thickness of the turbulent layer the zoom array has an advantage. This arises because the zoom is a slightly more centrally condensed array. Counter-intuitively the zoom can have lower phase noise even though it has larger maximum baselines than the dual ring.

6 Offset Centre Designs Offset centre zoom array designs with the most densely packed parts to the array close to one of the sites identified by Radford and Butler as flat and smooth have been produced (see [Offset Zoom Array](#) .). The beam shapes and uv coverages remain of high quality. No similar design has yet been produced for the dual ring concept. Because its antenna pattern is smoothly increasing in density with decreasing radius there are reasons to believe that such offset designs would give better uv coverage and beams than dual ring designs.

All the above points depend on the zoom array geometry and not on how it operated (i.e. 'burst' or 'continuous' reconfiguration) in addition there are some extra advantages that the zoom has if operated in continuous reconfiguration mode.

7. Matched Resolution and High Observing Efficiency Continuous reconfiguration mode allows observations in different line transitions to have exactly matched resolution. Because the need to taper the data is reduced the observing efficiency (i.e. total used observing baseline hours) is maximised.

8. Operational Advantages A small crew can be permanently employed doing reconfiguration, rather than requiring intermittent large amounts of personnel to execute big moves. All reconfigurations can be made in the mornings before (winter) winds get too large. This mode 'spreads the risk' of the impact of weather related reconfiguration delays compared to one in which infrequent big moves are made; minimising impact on personnel schedules.

Point 7 is probably less than compelling than point 8, and the choice between 'burst' and 'continuous' reconfiguration modes will and should be determined by operational concerns.

After starting from quite different positions the two proposed designs have converged quite

considerably. The ring design is now a set of five concentric circles each different by a factor of 2.1 apart in size, the outer two of which are occupied at any one time. The zoom array can be considered as a much larger number of concentric circles of antennas with many more outer circles occupied simultaneously. The dual ring is in effect itself a 'zoom' array except that it only zooms over fixed scales of 2.1. Given the convergence that has occurred it is not surprising that there are no highly dramatic differences between the two array designs. However in each of the eight points above the zoom array seems to have an advantage. There seems in contrast to be no compelling reasons to built in fixed scales into an array when a scale free array exists - these fixed scales simply reduce flexibility and add inhomogeneities into the uv point radial distribution. The only justification for placing antennas on rings is to improve the coverage of the very shortest baselines, but we have shown by suitably populating that the pads the zoom array can actually have better short baseline coverage than the dual ring arrays (see Table 1 and Figure 7).

7. Future Work

Future work should focus on producing a detailed site plan. At the next level of complexity plans for roads and conduits should be built in. The next iteration of the design should also probably allow smaller baselines. The dual ring arrays have ratios of maximum to minimum baseline lengths of order 40. The zoom configurations have ratios of between 40 and 70. In comparison the VLA with 2.4 times fewer antennas has a ratio of 45 in its non-hybrid arrays. Modifying the zoom array to allow baselines down to 30m in A array and 15m in B-array might be desirable. Another area which requires more work is the 12km array and the interface with the present A-array. Site restrictions mean that the 12km array must be a ring, in which case its resolution will be more than 4 times larger than the present A-arrays which are still somewhat centrally concentrated (the resolution ratio will be closer to 5). In the zoom design by adding about 16 pads to the present A-Array design, so that virtually all antennas could be put around the perimeter of the 3km area, an A+ configuration with 30% higher resolution than the present A could be produced. Such an array would help bridge the gap to the 12km array.

The new designs must be optimised, and its not clear we have the best tools yet for this optimisation. It seems that there are strong indications that optimising the beam shape is the best way to ensure imaging quality. Elaborations of the Kogan algorithms that optimise the image sidelobes for observing gaussians of all angular sizes is one possible approach, This metric incorporates beam quality and range of baseline length sampled into one single metric.